Annals of 3D Printed Medicine 17 (2025) 100187

Contents lists available at ScienceDirect

Annals of 3D Printed Medicine

journal homepage: www.elsevier.com/locate/stlm

Research paper

Multi-resin 3D printing of radiopaque customized artificial tooth for revolutionizing preclinical training on root canal treatment

Yi-Ching Ho [a,b], Wan-Rong Jiang [c], Yulius Shan Romario [d], Chinmai Bhat [d], Maziar Ramezani [e], Cho-Pei Jiang [d,f,g,*]

[a] Department of Stomatology, Taipei Veterans General Hospital, No. 201, Sec. 2, Shipai Rd., Beitou District, Taipei City 11217, Taiwan
[b] Department of Dentistry, National Yang Ming Chiao Tung University, No. 1001, Daxue Rd, East District, Hsinchu City 30010, Taiwan
[c] Epsom Girl Grammar School, Silver Road, Epsom, Auckland 1023, New Zealand
[d] High-value Biomaterials Research and Commercialization Center, National Taipei University of Technology, Taipei, Taiwan
[e] Auckland University of Technology, 55 Wellesley Street East, Auckland CBD, Auckland 1010, New Zealand
[f] Department of Mechanical Engineering, National Taipei University of Technology, No. 1, Section 3, Zhongxiao E Rd, Da'an District, Taipei City 10608, Taiwan
[g] Oral Medicine Innovation Center, National Yang Ming Chiao Tung University, No. 1001, Daxue Rd, East District, Hsinchu City 30010, Taiwan

ARTICLE INFO

Keywords:
Dental model
Multi-material 3D printing
Root canal
Preclinical endodontic training
Radiopacity

ABSTRACT

Objectives: This study aims to 3D print customized dental models using a multi-material 3D printer that can mimic natural human teeth. The model consists of a detailed tooth with adequate radiopacity and pulp cavity which will be used for preclinical endodontic training.
Methods: A radiopaque resin with varying barium sulfate ($BaSO_4$) ratios was synthesized to optimize printability and radiopacity. The artificial tooth with a pulp cavity was created from micro-computed tomography (micro-CT) data and printed using a multi-resin 3D printer, employing clinical A2 resin (AA-Temp) for the tooth body and soft red resin for the pulp. Periapical radiography evaluated the radiopacity, and the effect of $BaSO_4$ on resin viscosity and hardness was measured.
Results: Experimental results show that adding a 10% weight ratio of $BaSO_4$ in A2 resin can obtain the highest radiopacity of the printed tooth. Furthermore, the study successfully fabricated incisor and molar tooth models for preclinical endodontic training which closely matched the natural human tooth in terms of appearance, size, and shape.
Originality and significance: The multi-material 3D printing technology that is capable of fabricating hard and soft parts of the tooth is self-developed. Furthermore, two training models were successfully framed for students to get hands-on experience in root canal treatment of incisor and molar teeth. The enhanced confidence gained by training on the 3D-printed tooth that closely matches the characteristics of a natural human tooth would increase the clinical success rate.

1. Introduction

Endodontic therapy is one of the notable clinical therapeutics that deals with the treatment of pulpal disease caused by caries, trauma, or periodontal conditions. The major focus of this treatment involves the complete removal of debris and infected dentin from the root canal [1]. This treatment is clinically complicated due to the thin and complex root canal which makes it difficult for an amateur dentist to completely clean and shape the root canal. Thus, this requires extensive preclinical endodontic training for dentists to gain expertise and increase the clinical success rate. However, the scope of preclinical training so far has been limited due to the unavailability of natural teeth. With the advent of additive manufacturing (also known as 3D printing), it is now possible to fabricate an artificial tooth mimicking the natural ones [2]. In this regard, a recent study proposed the combination of cone-beam computed tomography (CBCT) and multi-jet printing technology to generate accurate artificial teeth. The artificial teeth were similar to natural teeth and can be used as a good tool for endodontic training and root canal filling [3]. Moreover, recent advancements in 3D printable materials have significantly enhanced dental practices over the past decade. Understanding the current status of 3D printing in dentistry is essential for translating its applications from the laboratory to the clinical setting [4,

* Corresponding author.
E-mail address: jcp@mail.ntut.edu.tw (C.-P. Jiang).

https://doi.org/10.1016/j.stlm.2025.100187
Received 23 September 2024; Received in revised form 20 November 2024; Accepted 18 December 2024
Available online 10 January 2025

5]. Software such as Mimics has become an essential tool to visualize abnormal anatomy, detect root canal morphology, and reconstruct the model for 3D printing applications [6]. One of the studies proposed a workflow that used Digital Imaging and Communications in Medicine (DICOM)-data and 3D printing technology for an interdisciplinary training model. The results demonstrate that 3D printing technology provides dental schools with new possibilities by enabling the creation of customized teaching models tailored to their specific curricula [7]. The literature indicates that 3D printing can provide customized artificial teeth for dental clinical courses, enabling students to simulate various tooth shapes and surgical scenarios, thereby enhancing their preclinical proficiency [8].

The 3D-printed artificial teeth should mimic the mechanical properties of the natural teeth to simulate the real tactile sensation during preclinical training. Natural teeth are composed of several different layers, each with its own unique structural geometries and mechanical properties. Enamel is the outermost layer of the tooth, composed primarily of hydroxyapatite, owing approximately 80–100 GPa of Young's Modulus and the Vickers hardness of around 300–500 HV [9,10]. Dentin lies beneath the enamel and is softer with a relative hardness value of 50–70 HV and ~18 GPa of Young's Modulus [11–13]. The cementum that covers the tooth root has Young's Modulus and hardness of around 10–15 GPa and 40–60 HV, respectively. The pulp is the innermost part of the tooth and does not contribute to the tooth's hardness or strength [14, 15]. An anatomical ceramic root canal for endodontic training was prepared indirectly using a ceramic shaping technique. The process involves 3D printing resin to create a pulp, placing it in a mold, casting it with slurry, and then sintering the mixture [16]. To mimic the appearance, barium sulfate ($BaSO_4$) powder was mixed with photocurable resin to 3D print an artificial tooth with radiopaque properties. The 3D-printed replica was considered easier to handle for preclinical endodontic training compared to that of extracted human teeth, as the resin's hardness made the preparation simpler. In contrast, the filling of the replica's root canals was judged to be very comparable to that of real teeth [17]. Students greatly appreciated the 3D-printed tooth for standardizing endodontic training but noted that its radiopacity and material hardness (i.e. resin's hardness) were not similar to those of extracted teeth [18]. Therefore, improving 3D printing techniques to directly fabricate customized artificial teeth with appropriate radiopacity and hardness is of prime importance. This will increase the level of mimicking with the actual extracted teeth, thereby enhancing the preclinical endodontic training.

The primary goal of this study is to make 3D-printed customized teeth more suitable for endodontic training. This can be achieved with appropriate mechanical properties, radiopacity, and dimensional precision. Most 3D printing resins are not inherently radiopaque. To achieve radiopacity, powders such as titanium dioxide (density: 4.23 g/cm^3), quartz (density: 2.65 g/cm^3), zirconia (density: 5.68 g/cm^3), bismuth oxide (density: 8.9 g/cm^3), barium sulfate (density: 4.5 g/cm^3), and ytterbium trifluoride (density: 7.18 g/cm^3) can be added to the resin [19–21]. Regarding the physical appearance, there is no significant difference in cleaning efficiency between different colors when using denture cleansers [22]. The color of the resin for artificial teeth cannot be transparent and thus, dental A2 color is the most common choice. Furthermore, if the pulp is also A2 in color, it will be difficult to visually determine whether the access opening reaches the pulp chamber. Razavian et al. [23] proposed a manual process to make artificial teeth containing simulated pulpal tissue. Additionally, the pulp should have soft characteristics. Thus, to produce artificial teeth with both hard and soft properties in the same printing process, a multi-resin 3D printing method is necessary.

The multi-resin 3D printing method using VAT photopolymerization technology was first applied to the creation of complete dentures. This method allows for the simultaneous printing of teeth and gingiva on a single printer, eliminating the need for positioning, alignment, and bonding steps during post-processing. As a result, it saves time, reduces human errors, and achieves higher accuracy [24]. To apply this technology for the fabrication of customized artificial teeth, it needs to handle two different photocurable resins (one to mimic hard material with mechanical properties similar to enamel and dentin and the other to mimic soft material with properties akin to pulp). To achieve the desired radiopacity of artificial teeth, the density of the powder added to the photo-curable resin needs careful consideration. An appropriate density and powder particle size will ensure good suspension, preventing settling and maintaining homogeneity during the printing process [25]. This study aims to utilize multi-resin three-dimensional printing technology to produce customized artificial teeth that are radiopaque and possess the mechanical properties of both enamel/dentin and pulp.

2. Method and materials

2.1. Model creation

The process of creating the customized artificial tooth model using an extracted tooth, code-named teeth-07, is shown in Fig. 1. At first, a micro-computed tomography (micro-CT) scan is performed on teeth-07 to obtain the DICOM image file, as shown in Fig. 1(a). The open-source imaging software, 3D Slicer, is used to visualize the DICOM file in 3D modeling, as shown in Fig. 1(b). The density of signal points needs to be adjusted for accurate modeling. Fig. 1(c) shows that excess parts are displayed when the density is too high, while an incomplete 3D model results if the density is too low. The density needs to be adjusted until the cross-sectional part is completely filled for 3D modeling, as shown in Fig. 1(d). After the model is exported to STL files, two files can be obtained: one is the tooth model without the pulp part (Fig. 1(e)), and the other is the pulp model, as shown in Fig. 1(f).

2.2. Material preparation

2.2.1. Photocurable resins

This study utilized three types of resins for the experiments. The artificial tooth was made from an A2 color resin (AA Temp, Enlighten Co., Taipei, Taiwan) and a transparent resin (DD Guide, Enlighten Co., Taipei, Taiwan). Both the resins, noted as tooth resin, are biocompatible acrylic-based materials known for their high strength, high hardness, and low shrinkage rate. The material of the pulp chamber consisted of a transparent PU-like soft resin (GC3D-ESK), noted as pulp resin, with added red dye to facilitate easy observation. Due to the opacity of the A2 resin, a transparent light-curing resin DD guide was selected to allow for the internal pulp space of the printed artificial teeth to be visible to the naked eye.

2.2.2. Addition of powder to achieve radiopacity

Barium sulfate ($BaSO_4$) powder was chosen as the radiopaque material. Different concentrations of the powder (2, 5, 8, 10, and 15 wt.%) were added to the two resins to observe changes in viscosity, hardness, ultimate tensile strength (UTS), and radiopacity. Notably, $BaSO_4$ powder requires surface modification to prevent nonhomogeneous dispersion, rapid precipitation, and aggregation within the resin. Therefore, a titanate coupling agent was used to modify the barium titanate powder. The modification process involves initially dispersing the powder in a solvent (ethanol) solution, followed by the addition of 1 wt.% coupling agent for modification. At first, the barium sulfate powder is placed in an oven at 120 °C to remove moisture. Then, the powder is mixed with ethanol in a 1:1 ratio, and 1 wt.% coupling agent is added. The mixture is then placed in a barrel for ball milling for 2 h at a speed of 200 RPM. After the ball milling, the mixture is returned to the oven to evaporate the ethanol thus, completing the surface modification of the barium sulfate powder. Finally, the modified barium sulfate powder is added to the photocurable resin in the desired weight percentage, along with a suitable weight percentage of polypropylene glycol (PPG) dispersant to enhance the dispersion and bonding strength of the barium sulfate in the

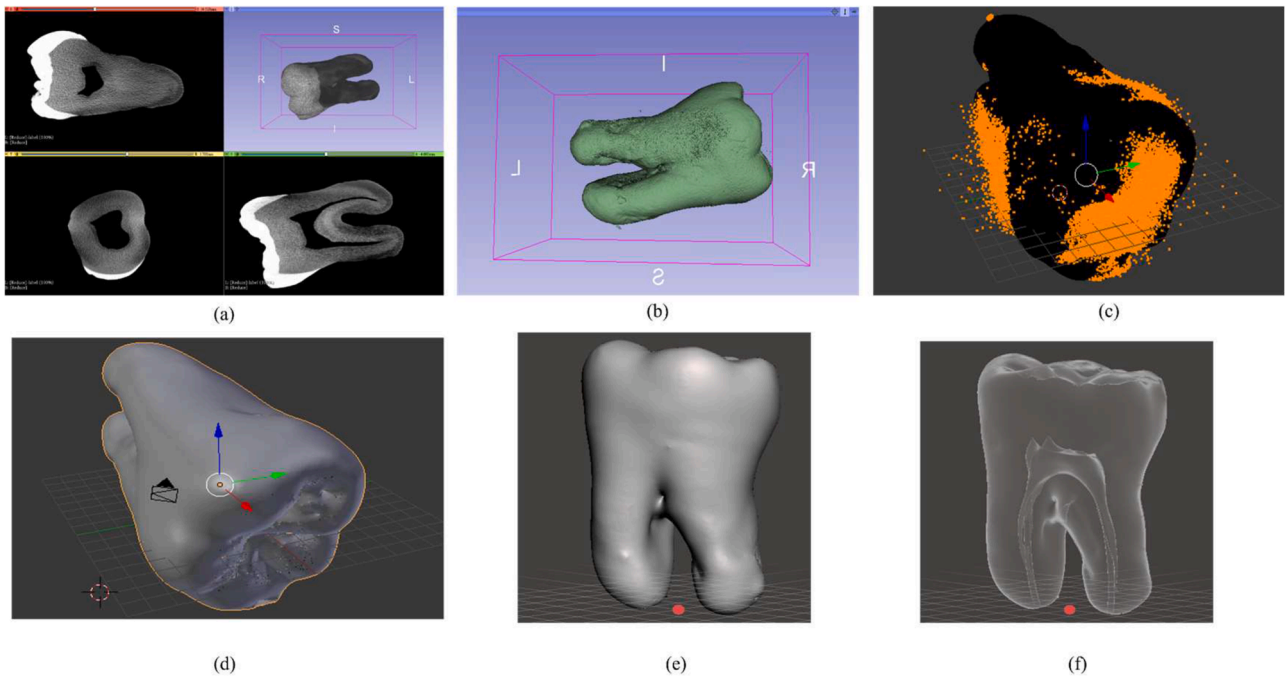

Fig. 1. Process of Creating the Customized Artificial Tooth Model. (a) DICOM image from a micro-CT scan. (b) 3D visualization. (c) Excess parts are displayed when the signal point density is too high. (d) Fully filled cross-section after adjusting signal point density. (e) Exported STL tooth model without pulp (f) Exported STL tooth model with pulp.

resin.

2.3. Multi-resin 3D printing process

The multi-resin 3D printing process used in this study employs a digital light processing (DLP) projector to expose the layer pattern from the bottom of the build platform. Fig. 2(a) shows the build chamber which consists of two resin tanks filled with tooth resin (AA temp or DD guide) and pulp resin (GC3D-ESK), respectively. Fig. 2b illustrates the working principle of the multi-resin 3D printing system customized for this study. This research uses two different tooth resin materials: AA Temp and DD guide. Each resin is contained in separate vats, with Vat A filled with AA Temp and Vat B with either DD guide + $BaSO_4$ or GC3D-ESK depending on the benchmark (explained in the subsequent section of the manuscript). A cleaning vat is positioned between the two vats, developed to clean the object after each layer is printed.

The process begins with printing in Vat A, followed by a cleaning step. The platform then rotates 90° to Vat B for printing the other resin. Fig. 2c shows the construction and operation of the cleaning chamber, which consists of three perforated sleeves. The sleeves on the right and left sides dispense pressurized alcohol for cleaning, while the middle sleeve sprays pressurized air to dry the object, ensuring no alcohol residue remains on the surface. Residual alcohol can increase the likelihood of delamination between layers. The cleaning chamber also has an outlet to flush away the used alcohol.

Additionally, a perfect cleaning system can prevent the two printing materials from contaminating each other. The build platform is fastened on a rotating lift shaft. Compared to traditional manual assembly or material injection methods, this printing method has the advantage of being fully automated and free from human error.

The printing process involves importing the two STL files, the tooth model with the pulp cavity and the pulp model, into the slicing software, as shown in Fig. 3(a). Before slicing, it is ensured that the necessary support structure is created, as illustrated in Fig. 3(b). It is recommended that the diameter of the support bar be 0.4 mm and the contact diameter be 0.2 mm to minimize visible defects on the surface of the printed artificial teeth after the removal of supports. Next, the slicing process converts the 3D image into a 2D projection image, as shown in Fig. 3(c). This 2D image is then transferred to a multi-resin 3D printer for printing, as depicted in Fig. 3(d). This layer-wise printing process repeats until the fabrication of the artificial tooth. Fig. 3(e) shows the final printed tooth after the removal of supports.

2.4. Mechanical property measurement

The modified barium sulfate powder acts as an X-ray absorber during radiography and thus, was added to AA Temp and DD Guide photocurable resins in different weight proportions. Printed test specimens were then used to measure mechanical properties, including tensile strength, hardness, and viscosity coefficient. Tensile strength testing follows ASTM E8/E8 M specifications and is conducted on printed tensile test specimens (WM-02 KEUTM, World Metrology Co., Taiwan). Hardness is measured using cylindrical test specimens with a diameter of 30 mm and thickness of 10 mm. The printed hardness specimens are measured at 12 points to determine the average hardness (HMV-G Series, Shimadzu Co., Japan). Additionally, six test specimens are printed for each experimental material formula to ensure data reliability. Viscosity coefficient measurements were performed using a high-viscosity rheometer (DV3THA, Ametek Brookfield).

2.5. Printing benchmark testing and radiopacity

In this study, two benchmark training modules were designed for dentists to practice the surgical procedure and design standard operating procedures (SOPs). In the first benchmark shown in Fig. 4a, the incisor crown is printed using AA temp material, while the incisor root is printed using DD guide + $BaSO_4$. Due to the transparency of the DD guide material, dentists can perform root canal treatment and check if the cleaning and shaping procedure is complete. Due to the ease of printing the artificial tooth, the dentists can get a repeated experience of the procedures. The second benchmark training module consists of following the standard root canal treatment procedures. Fig. 4b shows the molar tooth model with an internal pulp made up of soft material (GC3D-ESK). Since the actual tooth is non-transparent, it is necessary to

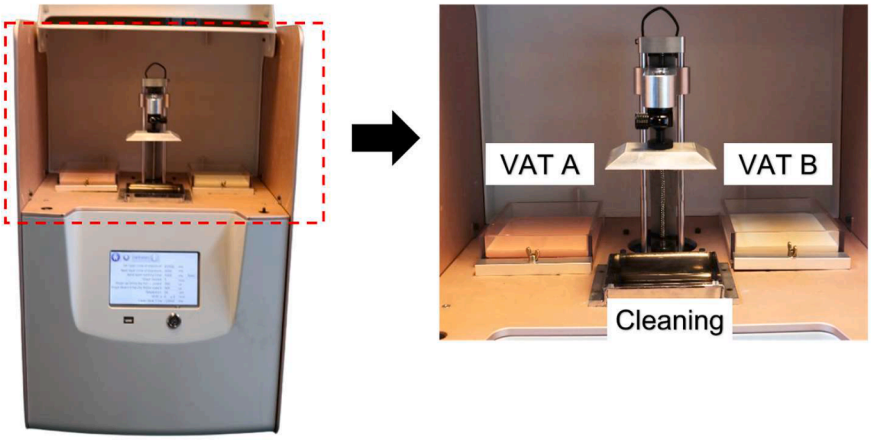

(a)

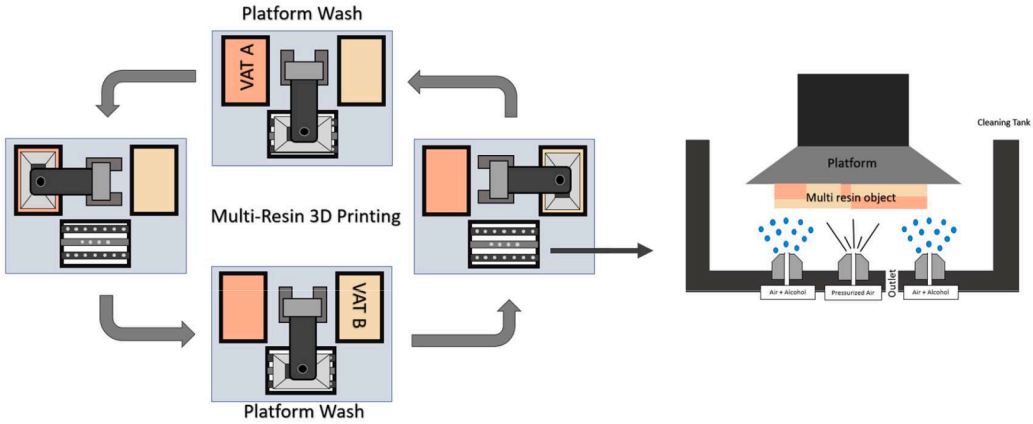

(b)

Fig. 2. Multi resin 3D printing (a) Multi resin 3D printing machine overview (b) schematic diagram of working principle and the cleaning system.

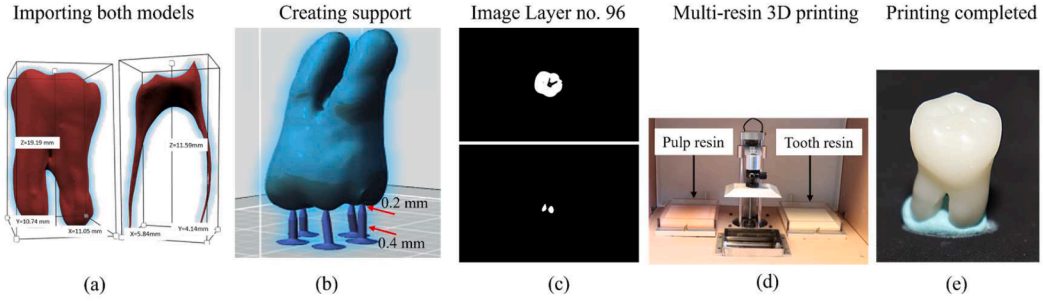

Fig. 3. Workflow for multi-resin 3D printing of artificial teeth. (a) Importing tooth and pulp STL files, (b) creating support structures, (c) slicing process, (d) dual resin printing process, and (e) after post-processing.

take radiographs to ensure the working length during root canal treatment. This procedure is critical for cleaning and shaping the root canal. Thus, in this module, dentists will practice root canal treatment of a natural tooth-mimicked model with the standard clinical procedures.

3. Results

3.1. *Effect on printing parameters, mechanical properties, and radiopacity with the addition of $BaSO_4$*

The slicing thickness was fixed at 50 μm for both AA temp and DD guide resins, as shown in Table 1. The effective exposure time (EET) was measured to ensure that the cured thickness exceeded twice the slicing

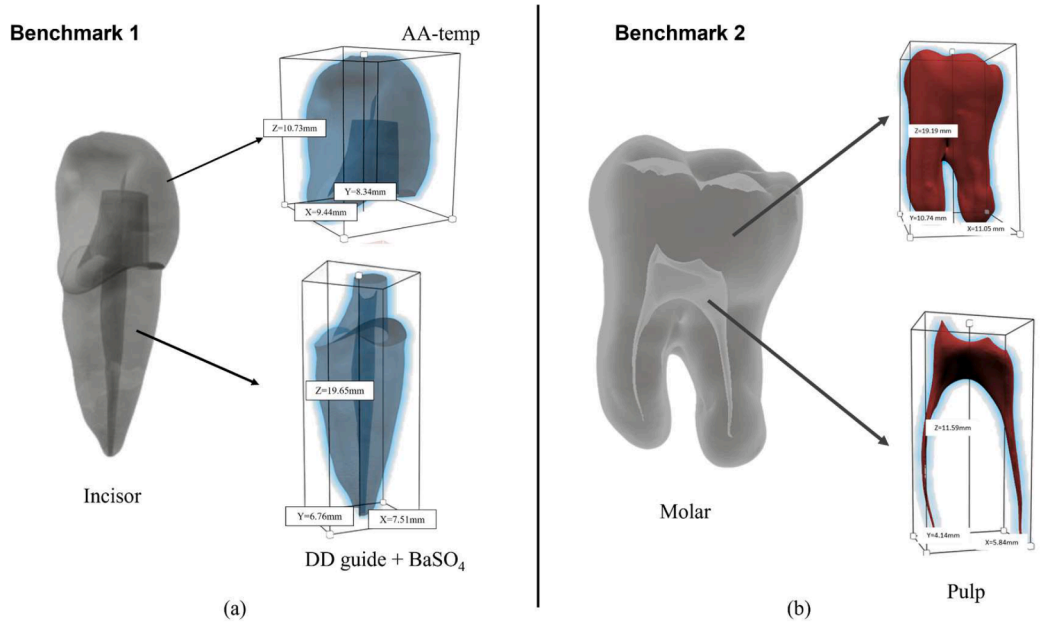

Fig. 4. Printing benchmark model (a) incisor (b) molar.

Table 1
Printing parameters for each resin.

	AA temp (A2 color)	DD guide	GC3D-ESK
Layer thickness (μm)	50	50	50
EET (s)	1.3	1.5	3
+ $BaSO_4$ (2 wt.%)	1.3	1.5	
+ $BaSO_4$ (5 wt.%)	1.3	1.7	
+ $BaSO_4$ (8 wt.%)	1.5	1.7	N/A
+ $BaSO_4$ (10 wt.%)	2.3	2.0	
+ $BaSO_4$ (15 wt.%)	2.7	2.3	

thickness, preventing delamination after printing. The printing parameters for these resins are listed in Table 1. When AA temp and DD guide resins do not include $BaSO_4$ powder, the effective exposure times are 1.3 s and 1.5 s, respectively. The more $BaSO_4$ powder added in resin, the longer the effective exposure time required for each layer. When $BaSO_4$ powder constitutes 15 wt.% of the resin, the exposure times for AA temp and DD guide are 2.7 s and 2.3 s, respectively. The exposure time for soft resin (GC3D-ESK) was 3 s.

Fig. 5(a) shows that varying the weight proportions of modified $BaSO_4$ powder minimally affects the viscosity coefficient of the two tooth resins. For DD guide resin, the viscosity coefficient increases from 210 cPs to 275 cPs with the increasing weight percentage of $BaSO_4$. The highest viscosity coefficient of 275 cPs does not affect the shear force generated when the material is backfilled into the vacancy or when the platform is lifted out of the vat during the printing process. For AA temp resin, which is an A2 color resin with sufficient filler added to control the color, resulting in an initial viscosity coefficient of 455 cPs. As more $BaSO_4$ powder is added, the viscosity coefficient increases. At a concentration of 15 wt.% $BaSO_4$ powder, the viscosity coefficient reaches 550 cPs. During printing, this requires an increase in backfill time by approximately 2 s.

The hardness value increases with the amount of modified $BaSO_4$ powder added. Fig. 5(b) shows that the original hardness of the DD guide and AA temp are 210 HV and 455 HV, respectively. Fig. 5(b) also illustrates that the impact of adding modified $BaSO_4$ powder on the DD guide is greater than the impact of adding it to AA temp.

Radiopacity is a crucial characteristic in dental materials, especially for performing root canal treatments. It allows students to observe surrounding tissues in radiographic images during training easily. This study analyzes the effect of adding $BaSO_4$ powder to tooth resin on its radiopacity properties. Fig. 6 illustrates the comparison of incisor tooth models fabricated using tooth resin with varying concentrations of $BaSO_4$.

Fig. 6a shows the model fabricated with pure DD guide resin, while Figs. 6b and 6c are fabricated with DD guide adding 2% and 5% $BaSO_4$, respectively. The results indicate that the radiopacity is relatively low, with the outline and internal structure of the fabricated incisor appearing faint and unclear. In Figs. 6d, e, and f, a significant improvement in radiopacity characteristics can be observed. Among these compositions, the 10% $BaSO_4$ addition shows the best results. The fabricated tooth structure is very clear, and the internal anatomy is well-defined. However, with a 15% $BaSO_4$ addition, the outside structure of the fabricated incisor tooth is not visible at all.

3.2. *Preclinical endodontic training with the first benchmark module*

3.2.1. *Case 1*

Fig. 7(a) presents an incisor dental tooth model fabricated using a multi-material 3D printer. The root portion is made with DD guide resin and $BaSO_4$ to enhance radiopacity. The crown part of the model is fabricated using AA-temp material due to its aesthetic properties, mimicking the natural color and translucency of natural dental crowns.

The radiographic images in Fig. 7(b) reveal fine details of both crown and root structures, including internal canal morphology. These details are crucial for supporting preclinical training, helping students understand the complexities, and practicing accurate treatment techniques. The combination of different materials in multi-resin 3D printing enables the mimicking of natural tooth properties thereby providing a more realistic training experience. Additionally, the customization capability of multi-resin 3D printing allows for the creation of tooth models that simulate various clinical scenarios effectively.

Figs. 8(a) and (b) illustrate the front and back views of a 3D-printed training model designed for preclinical endodontic training in root canal treatment, respectively. Fig. 8(c) shows the radiographic image of the radiopaque artificial tooth. The visual and tactile similarities to real teeth aid in the development of enhanced clinical skills among students.

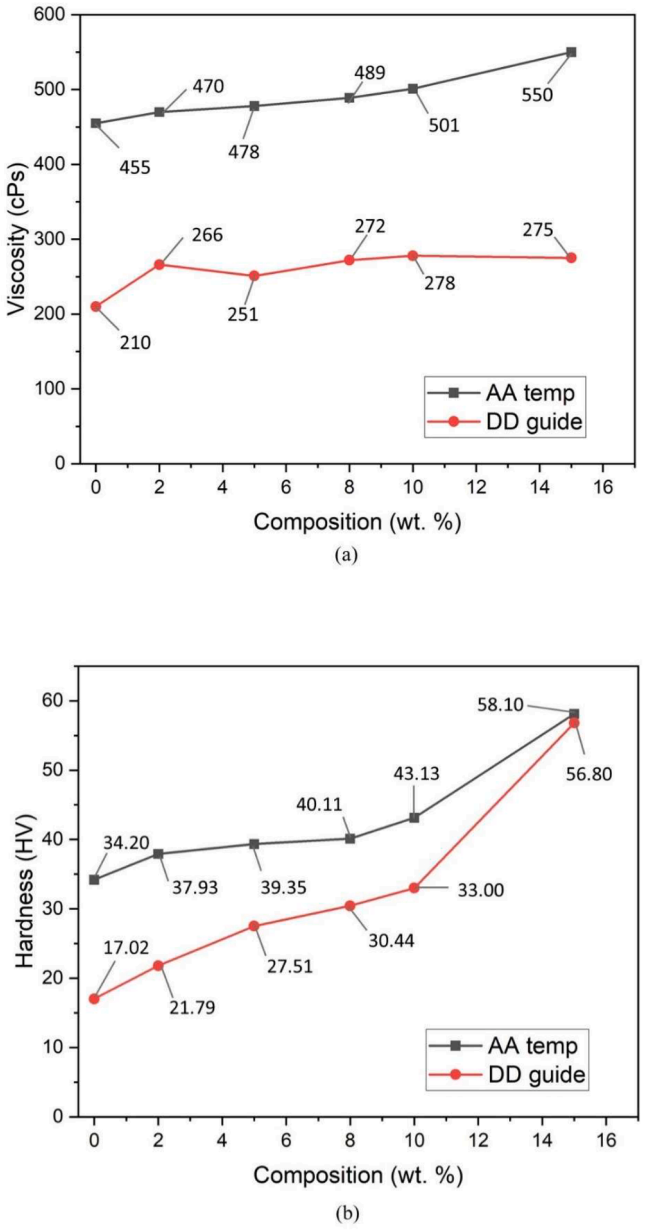

Fig. 5. The impact of modified $BaSO_4$ powder addition on tooth resins. (a) viscosity and (b) hardness.

3.2.2. Case 2

Fig. 9 illustrates various configurations of 3D-printed artificial molar tooth designed for preclinical endodontic training. The different configurations include a tooth made with AA-Temp resin containing $BaSO_4$ and a pulp chamber (Fig. 9(a)), a tooth made with DD-guide resin with a pulp chamber (Fig. 9(b)), a DD-guide resin tooth with a dyed red pulp chamber (Fig. 9(c)), and cross-section of the tooth to observe the pulp structure (Fig. 9(d)).

Fig. 9(a) depicts a tooth fabricated using AA-Temp resin with the addition of $BaSO_4$ to enhance radiopacity, along with a realistic pulp chamber. These models aim to replicate the natural tooth structure, enabling students to practice on materials that closely simulate the hardness and radiographic characteristics of natural teeth. The addition of $BaSO_4$ ensures the visibility of the tooth during radiographic imaging, which is important for practical procedures and assessing the working length of root canal treatments. The internal pulp chamber adds another level of realism, aiding students in accurately identifying the pulp chamber and root canal, thereby improving their precision and confidence in clinical practice.

Fig. 9(b) shows a DD-guide resin with an uncolored pulp chamber, while Fig. 9(c) displays a red-colored pulp chamber within the DD-guide resin tooth. The use of red dye in the pulp chamber is highly beneficial for educational purposes as it offers a distinct visual indication of the pulp's location. This feature helps students easily identify and access the pulp chamber during endodontic procedures. The bright color contrast facilitates the identification of the pulp chamber and ensures that students can efficiently eliminate all colored material, replicating comprehensive root canal cleaning and shaping procedures in real root canal treatments. Fig. 9(d) shows the tooth cut in half to observe the internal pulp structure. This cross-sectional view is instrumental in providing a comprehensive understanding of the tooth's internal anatomy. It allows students to visually inspect the pulp chamber and understand its spatial relationship with the surrounding tooth material.

4. Discussion

4.1. Effect of printing parameters, mechanical properties, and radiopacity with $BaSO_4$ addition

The addition of $BaSO_4$ increased the exposure time due to the reduced transparency of the resin, which hindered UV light penetration and prolonged the curing process. This finding aligns with prior research, which also reported that higher filler content reduces resin transparency [26]. Despite the increased curing time, the overall printing duration remained practical for dental applications, as a complete artificial tooth could still be printed within 2.5 h. The extended exposure times observed are not a limiting factor, with cleaning time between resin switches being the most time-intensive process.

The minimal impact of $BaSO_4$ addition on the viscosity of DD guide resin is likely due to the originally this resin was a transparent resin with no filler, as noted in similar studies on adding $BaSO_4$ [27–29]. The increase in viscosity for AA temp resin, containing pre-existing fillers, aligns with findings that high filler content amplifies viscosity. Despite this, the increased backfill time of 2 s remains manageable for practical applications. The increase in hardness with $BaSO_4$ addition supports the notion that the fillers enhance the mechanical properties of materials [30–32].

Radiopacity improvements with 10% $BaSO_4$ align with the requirements for endodontic applications, where clear visualization of internal structures is vital. However, the loss of external visibility at 15% $BaSO_4$ highlights a trade-off between radiopacity and optical clarity. These findings echo previous work emphasizing the need for optimal filler concentrations to balance functional and aesthetic properties. The superior radiopacity at 10% $BaSO_4$ facilitates better preclinical training outcomes by enhancing the ability to assess techniques and recognize errors in radiographic imaging.

4.2. Preclinical endodontic training with the first benchmark module

4.2.1. Case 1

The integration of $BaSO_4$ in the root section of the tooth model enhances radiopacity, ensuring visibility in radiographic images, crucial for endodontic training. These findings are consistent with earlier research emphasizing the importance of radiopacity in dental models for accurately simulating clinical conditions [30,33]. The use of AA-temp for the crown mimics natural aesthetics and it will enhancing the realism in training [34]. Multi-resin 3D printing's ability to replicate natural tooth properties underscores its potential for preclinical applications, as it provides a versatile platform for creating models tailored to diverse clinical scenarios [35,36].

4.2.2. Case 2

The configurations presented in Fig. 9 highlight the flexibility of 3D printing in producing dental models with distinct functional and

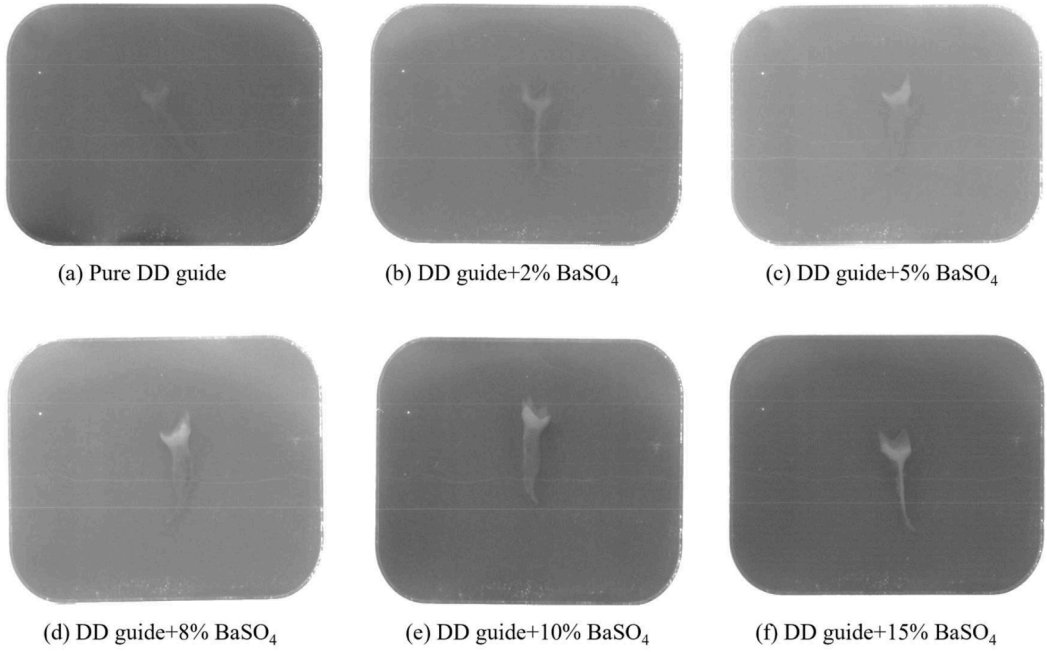

Fig. 6. The radiopacity impact of modified $BaSO_4$ powder addition on tooth resins.

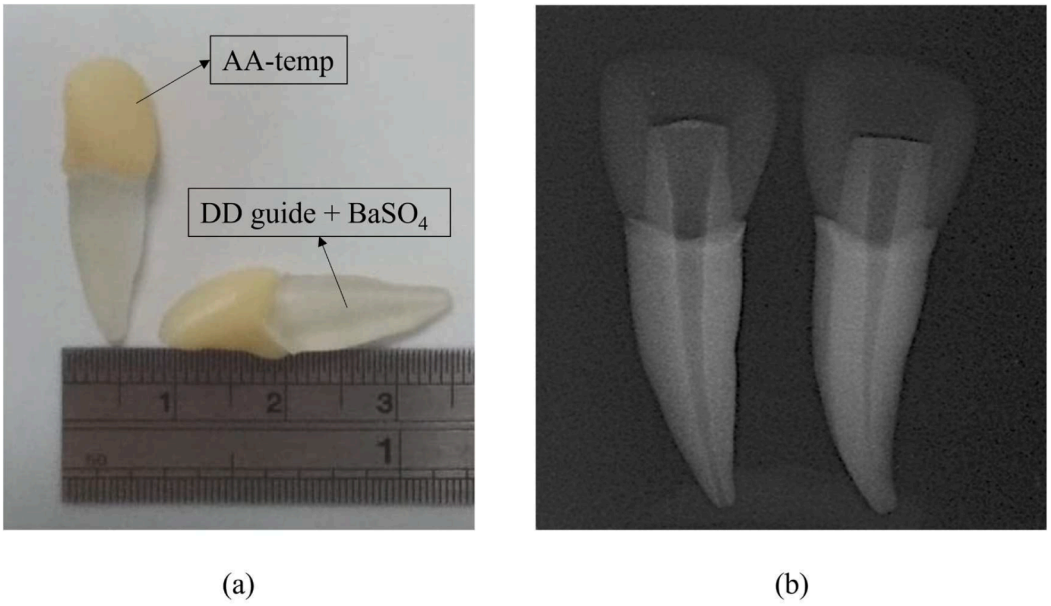

Fig. 7. The fabricated model using multi-resin 3D printing (a) incisor model (b) radiographic images (first benchmark training module).

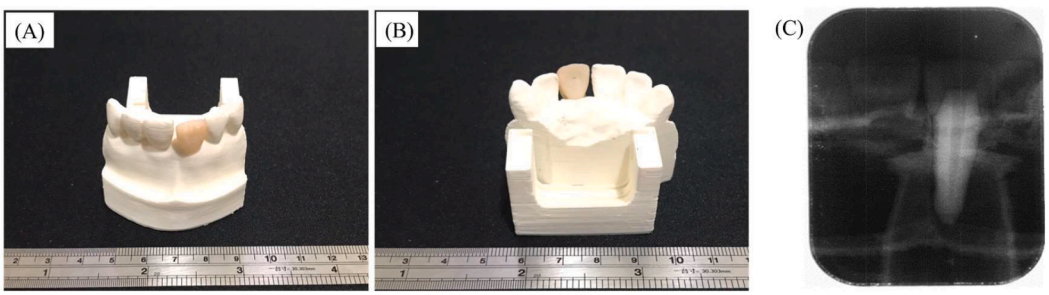

Fig. 8. Fabricated preclinical training tools (a) front view (b) back view (c) radiographic image.

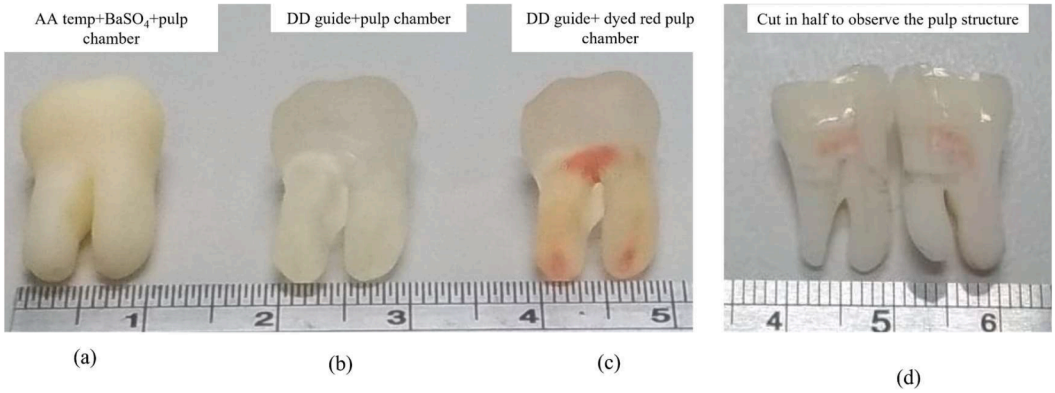

Fig. 9. The fabricated molar tooth model with varying resin using multi-resin 3D printing (a) AA temp+$BaSO_4$ (b) DD guide + pulp chamber (c) DD guide + dyed red pulp chamber (d) half cut of the molar tooth model.

educational features. The use of $BaSO_4$ in AA-temp resin (Fig. 9a) offers a balance between radiopacity and hardness, simulating natural tooth conditions for root canal practice. The incorporation of a red-dyed pulp chamber (Fig. 9c) aligns with pedagogical strategies for enhancing visual feedback, aiding students in identifying and eliminating target materials during practice. The cross-sectional model (Fig. 9d) provides an anatomical reference for students, improving spatial understanding of pulp structures. These features collectively improve precision, confidence, and skill acquisition in endodontic training.

5. Conclusions

Endodontic treatment is becoming more common these days due to the advancement of the medical and healthcare sectors. Amongst the various tooth restoration treatments, root canal treatment is the most common that patients often undergo. The technological advancement of additive manufacturing has been a promising tool in developing customized replicas that can be used for practice sessions for students (i.e. preclinical endodontic training). This study aims to develop customized dental tooth models mimicking natural human teeth and fabricate them with self-developed multi-material additive manufacturing (AM). The study successfully fabricated two tooth models (i.e. incisor and molar) using clinical grade resins: AA-temp and DD guide. To mimic the internal pulp, a soft clinical-grade pulp resin GC3D-ESK is used. The tooth resins are mixed with the optimized quantity of barium sulfate to match the radiopacity of the natural tooth. The study successfully evaluates the effect of barium sulfate on the viscosity and hardness of the tooth resins. The evaluation of viscosity was necessary to analyze the flowability of the resin in the developed 3D printer. Though this study tries to mimic the radiopacity of natural teeth, there is a greater scope for selecting adequate resin that can match the hardness value of natural teeth. With such a material, the students would feel the hardness of natural teeth while accessing the opening. Two benchmark training modules were designed for the preclinical training of the students:

1. Module 1 consisted of an incisor dental model wherein, the crown part was fabricated using AA-temp material due to its aesthetic properties, mimicking the natural color and translucency of natural dental crowns. The root part was made up of transparent DD guide + $BaSO_4$. The transparency of the root part facilitates the trainee to check the level of drilling to reach the pulp cavity which is quite hard with the natural teeth. The model was kept removable so that the training could self-assess the level of access open and get repeated training.
2. Module 2 consisted of a molar tooth model fabricated using AA-Temp resin with the addition of $BaSO_4$ to enhance radiopacity, along with a realistic pulp chamber. These models aimed to replicate the natural tooth structure, enabling students to practice on materials that closely simulate the hardness and radiographic characteristics of natural teeth. The internal pulp chamber adds another level of realism, aiding students in accurately identifying the pulp chamber, thereby improving their precision and confidence in clinical practice.

Declaration of competing interest

The authors declare that they have no known competing financial interests or personal relationships that could have appeared to influence the work reported in this paper.

Acknowledgment/Funding

This research was funded by National Science and Technology Council (NSTC) of Taiwan, grant number 111–2622-E-027 −028, 111–2221-E-027 −087 -MY2, L713110–18 and 112–2218-E-A49 −028. This work is also supported by the “High-value Biomaterials Research and Commercialization Center” of the Featured Area Research Center Program within the framework of the Higher Education Sprout Project by the Taiwan Ministry of Education (MOE).

Reference

[1] Elfarraj H, et al. Effects of endodontic root canal irrigants on tooth dentin revealed by infrared spectroscopy: a systematic literature review. Dental Mater 2024.
[2] Maleki T, et al. Mechanical and physical properties of splint materials for oral appliances produced by additive, subtractive and conventional manufacturing. Dental Mater 2024.
[3] Liang X, et al. 3D-printed artificial teeth: accuracy and application in root canal therapy. J Biomed Nanotechnol 2018;14(8):1477–85.
[4] Balhaddad AA, et al. Three-dimensional (3D) printing in dental practice: applications, areas of interest, and level of evidence. Clin Oral Investig 2023;27(6):2465–81.
[5] Kouhi M, et al. Recent advances in additive manufacturing of patient-specific devices for dental and maxillofacial rehabilitation. Dental Mater 2024.
[6] Costamagna P, et al. Endodontic treatment of a molar with peculiar anatomy: case study with CBCT and 3D printed model. J Contemp Dental Pract 2021;22(12):1477–82.
[7] Reymus M, et al. Development and evaluation of an interdisciplinary teaching model via 3D printing. Clin Exper Dental Res 2021;7(1):3–10.
[8] Romario YS, et al. Fabrication of translucent graded dental crown using zirconia-yttrium multi-slurry tape casting 3D printer. J Mech Behav Biomed Mater 2024:106406.
[9] Park S, et al. Mechanical properties of human enamel as a function of age and location in the tooth. J Mater Sci 2008;19:2317–24.
[10] Zaytsev D. Mechanical properties of human enamel under compression: on the feature of calculations. Mater Sci Eng: C 2016;62:518–23.
[11] Dejsuvan S, Sirimaharaj V, Wanachantararak S. Nanohardness and elastic modulus properties of enamel and dentin of primary molars in vitro, in people with various caries experiences, using a nano-indentation technique. CM Den t J 2021;42(1):93–100.
[12] Andrejovská J, et al. Hardness and indentation modulus of human enamel and dentin. Surface Interface Analy 2023;55(4):270–8.

[13] Mao Z, et al. Antagonist enamel tooth wear produced by different dental ceramic systems: a systematic review and network meta-analysis of controlled clinical trials. J Dent 2024:104832.
[14] Cleghorn BM, Boorberg NB, Christie WH. Primary human teeth and their root canal systems. Endod Topics 2010;23(1):6–33.
[15] Zhang Y-R, et al. Review of research on the mechanical properties of the human tooth. Int J Oral Sci 2014;6(2):61–9.
[16] Robberecht L, et al. A novel anatomical ceramic root canal simulator for endodontic training. Europ J Dental Educ 2017;21(4):e1–6.
[17] Reymus M, et al. 3D printed replicas for endodontic education. Int Endod J 2019; 52(1):123–30.
[18] Kolling M, et al. Students' perception of three-dimensionally printed teeth in endodontic training. Europ J Dental Educ 2022;26(4):653–61.
[19] Shannon A, et al. A radiopaque nanoparticle-based ink using PolyJet 3D printing for medical applications. 3D Print Addit Manufac 2020;7(6):259–68.
[20] Shannon A, et al. Assessment and selection of filler compounds for radiopaque PolyJet multi-material 3D printing for use in clinical settings. J Eng Med 2022;236 (5):740–7.
[21] Collares F, et al. Ytterbium trifluoride as a radiopaque agent for dental cements. Int Endod J 2010;43(9):792–7.
[22] Çevlik, E.T., G.A. Demetoğlu, and T. Toprak, Effect of denture cleansers on color stability of acrylic and composite artificial teeth. Curr Res Dental Sci. 34(1): p. 54–58.
[23] Razavian H, Hanjani K. A new teaching model with artificial teeth containing simulated pulpal tissue. Dent Res J (Isfahan) 2021;18(1):19.
[24] Jiang, C.-P., et al., Multiresin additive manufacturing process for printing a complete denture and an analysis of accuracy. 3D printing and additive manufacturing, 2022. 9(6): p. 511–9.
[25] Zakeri S, Vippola M, Levänen E. A comprehensive review of the photopolymerization of ceramic resins used in stereolithography. Addit Manufac 2020;35:101177.
[26] Jiang C-P, Romario YS, Toyserkani E. Development of a novel tape-casting multi-slurry 3D printing technology to fabricate the ceramic/metal part. Materials, 2023; 16(2):585.
[27] Romero-Ibarra IC, et al. Influence of X-ray opaque BaSO4 nanoparticles on the mechanical, thermal and rheological properties of polyoxymethylene nanocomposites. J Polym Eng 2012;32(4–5):319–26.
[28] Liu H, et al. Enhanced slag resistance of magnesia refractory castables with addition of BaSO4. Ceram Int 2020;46(15):24238–47.
[29] Polaskova M, et al. Modification of polyvinyl chloride composites for radiographic detection of polyvinyl chloride retained surgical items. Polymers (Basel) 2023;15 (3):587.
[30] Liu H, et al. Enhancing effects of radiopaque agent BaSO4 on mechanical and biocompatibility properties of injectable calcium phosphate composite cement. Mater Sci Eng: C 2020;116:110904.
[31] Li B, et al. Effects of nano-barium sulfate on the properties of polybutylece terephthalate/polyethylene terephthalate composites. ES Mater Manufac 2022;17: 83–91.
[32] Ju J, et al. Effect of BaSO4 on the compressive strength and reduction behavior of pellets. Metallurg Res Technol 2020;117(2):207.
[33] Liu H, et al. The ability of different irrigation methods to remove mixtures of calcium hydroxide and barium sulphate from isthmuses in 3D printed transparent root canal models. Odontology 2022;110(1):27–34.
[34] Jiang C-P, et al. Development of 3d slurry printing technology with submersion-light apparatus in dental application. Materials (Basel) 2021;14(24):7873.
[35] Dobroś K, Hajto-Bryk J, Zarzecka J. Application of 3D-printed teeth models in teaching dentistry students: a scoping review. Europ J Dental Educ 2023;27(1): 126–34.
[36] Mahrous A, et al. A comparison of pre-clinical instructional technologies: natural teeth, 3D models, 3D printing, and augmented reality. J Dent Educ 2021;85(11): 1795–801.